CHEMICAL ENGINEERING TRANSACTIONS
VOL. 52, 2016
A publication of AIDIC
The Italian Association of Chemical Engineering
Online at www.aidic.it/cet
Guest Editors: Petar Sabev Varbanov, Peng-Yen Liew, Jun-Yow Yong, Jiří Jaromír Klemeš, Hon Loong Lam

ISBN 978-88-95608-42-6; **ISSN** 2283-9216
DOI: 10.3303/CET1652071

Electrified Water Sprays Generation for Gas Pollutants Emission Control

Lucia Manna[a], Francesco Di Natale*[a], Claudia Carotenuto[b], Amedeo Lancia[a]

[a]University of Naples, Department of Chemical, Material and Production Engineering, P.le Tecchio 80, 80125 Napoli, Italy
[b]The Second University of Naples, Department of Information and Industrial Engineering, Via Roma 29, 81031, Aversa, Caserta, Italy
francesco.dinatale@unina.it

In this study, we investigated the induction charging of water sprays and the effect of electric field on the breakup mechanism of liquid sprays. Two different kind of hollow cone hydraulic spray nozzles were used. Our investigation aimed to estimate the Droplet Charge to Mass Ratio (D-CMR) and the dependence of breakup length on electric potential. The experiments revealed that the D-CMR increased with the potential until to a maximum, then started to decrease. At the same time, the breakup length decreased more than 0.5 cm compared to the uncharged value, suggesting that the electric field actually influenced the jet break-up dynamics. For $V<V_{max}$, an induction charging model and a fluid-dynamic one were adopted to compare the theoretical droplet specific charge to experimental one. The experimental data are well described with a corrective factor of 0.243 by the induction charging model.

1. Introduction

The electrostatic charging of sprays is a technique used to improve the dispersion of liquids in gas thanks to the coupling of electric forces with the hydrodynamic or aerodynamic forces adopted in the conventional hydraulic or air-assisted sprays. Besides, charged droplets have peculiar behavior that allows their deposition on target surface also against the conventional gravitational forces. For example, electrified sprays of pesticides can be used to wet both the upper and the bottom sides of leaves, thanks to the electrostatic attraction between the charged drops and the leaves surfaces, which are at ground potential (Law 2001). Application of electrified sprays spreads over different fields, from medicine to agriculture (Law 2001), to industrial process and air pollution control (Jaworek et al. 2006). Recently, electrified spray scrubbers were proposed as an alternative to conventional technologies (Di Natale and Carotenuto, 2015) for marine diesel engines emission control (Di Natale et al., 2013).
There are three main technological approaches to spray charging: exposure to corona ions; contact charging (i.e. electrospray) and induction charging. Induction charging is the best compromise between water throughput and charging level. In fact, electrospray is suitable for low flow rate applications, while corona tends to produce low charging levels.
Law (1978) pointed out that for induction charging to be effective, the fluid must be sufficiently conductive to allow charge movement in the time frame of droplet formation. Quantitatively, the charge relaxation time of the fluid, τ, must be smaller than the formation time of the droplet, τ_D, evaluable from the ratio of breakup length and velocity of liquid jet.
In this sense, thanks to its high conductivity, tap water may be a very good candidate for electrification. However, water is an ionic liquid and its physical properties are subject to substantial change in presence of electric field (Chaplin, 2009): on the overall, electrified spray of water are more instable than those of organic fluids. A side effect of this result is that electrified water sprays are scarcely studied in the pertinent literature. Cross et al. (2003) investigated the removal of particles electrically charged by means of an inductively charged water spray. It was estimated that the charging level of water decreased with the flow rate because of the lower residence time of liquid in electric field. On the contrary, the droplets charge reached a maximum,

Please cite this article as: Manna L., Di Natale F., Carotenuto C., Lancia A., 2016, Electrified water sprays generation for gas pollutants emission control, Chemical Engineering Transactions, 52, 421-426 DOI:10.3303/CET1652071

which was related to the occurrence of gas breakdown. Di Natale et al. (2015) performed experimental tests on a pilot scale wet electrostatic scrubber for gas cleaning and showed that water electrification could be reliably achieved and that interactions of oppositely charged droplets and particles could give substantial improvement of particle removal inside a water scrubber. Krupa et al. (2013) compared the spray current measured with a hollow cone spray and a full cone one at different voltages. The current increased with potential up to a maximum. The maximum value was higher for the hollow cone thanks to the different charge distribution on liquid jet. It was due to the diverse mechanism of jet disruption that led to finest droplets formation that could acquire higher charge.

One of the main assumption of these studies is the observation that water sprays electrified by induction mostly preserve their droplet size distribution regardless of the charging levels (Krupa et al., 2013). In our opinion, this evidence mainly indicates that secondary spray atomization remains largely unchanged by electrification, giving rise to similar droplets. Apparently, this imply that the primary jet breakup is unaffected by the application the electric field. Differently, Laryea and No (2004) studied the breakup spraying parameters as spray angle and breakup length by atomizing kerosene in a pressure-swirl hollow cone. The results underlined that break-up length and the spray angle changed with increasing the applied voltage and the operating pressure. These findings were related to the charging of droplets, because they repulsed each other modifying the spray trajectory and the equilibrium between electric and aerodynamic forces. The modifications of jet break up length and of primary atomization mechanism influence the charging level that can be actually achieved by induction processes. At the best of our knowledge, there is no evidence of such phenomena for induction electrification of water.

In this work, we report experimental results on the induction charging of water, with specific reference to the charge levels and the primary jet atomization characteristics associated to the exposure to electric fields of different intensities. The charging level of liquid drops was evaluated by the ratio of droplets current I_{drop} and the exerted flow rate Q_L:

$$\mathrm{D-CMR} = \frac{I_{drop}}{Q_L} \tag{1}$$

Experimental results are interpreted in light of two mechanistic models available in the pertinent literature, namely the LISA model (Ashgriz, 2011) for the jet breakup and the induction charging model of Artana et al. (1993) used to describe experimental droplet charging.

2. Materials and Methods

The lab-scale experimental rig was made by a prototype of Droplet Charging Unit (DCU). The experiments were performed with tap water whose conductivity was 0.750 S/m. The DCU was composed by a Teflon box 20 × 6.2 × 9 cm, placed on a supporting structure. On its left there was the high tension connection. Two cylindrical wires of 1 mm diameter and distant 130 mm extended out from the Teflon box to support the electrode. It was a smooth circular torus with internal diameter of 110 mm and external diameter of 130 mm. In the middle of the charging unit, there was a stainless steel cylindrical tube of 2 cm large at which the nozzle was connected. The tube height could be changed to modify the distance Z between the nozzle exit and the centre of the electrode. Except for the ring and the supporting sticks, all the structure was grounded. The high voltage was provided by a DC power supply. The liquid was sprayed using the volumetric pump and it was regulated through an inverter. The sprayed droplets were collected in a Faraday Cage in order to measure their current. The cage was a cylindrical enclosure formed by a mesh of iron filaments and both dimensions and position had been preliminarily optimized to reduce water losses during measurements and electrical interferences. A representation of the experimental assembly is showed in Figure 1.

Two Lechler hydraulic nozzles (model 216.364 and 216.404) were used. Hereafter they are indicated as Nozzle 1 and 2, respectively. Their geometric and hydrodynamic features as spray angle θ and orifice diameter D_0 are resumed in Table 1.

Two experimental investigations were performed. Firstly, the break-up length L_b and spray angles θ of nozzles were evaluated by optical tests as function of the applied voltage. Photos were taken with a NIKON P300 at 3 and 6 bar. The images were elaborated with the software Image Pro Plus®. An example of optical tests results is shown in Figure 2 for two applied voltages. The second investigation aimed to measure the charge acquired from sprayed droplets. The charging tests were executed at 3 and 6 bar and the distance Z was fixed as breakup length at 0 kV. The current of droplets I_{drop} was measured at the Faraday cage, following the method of D'Addio et al. (2013), that was tested for a lab scale unit (D'Addio et al., 2014) and applied to a pilot scale WES unit in Di Natale et al. (2015). The droplet charge to mass ratio was calculated according to Eq(1).

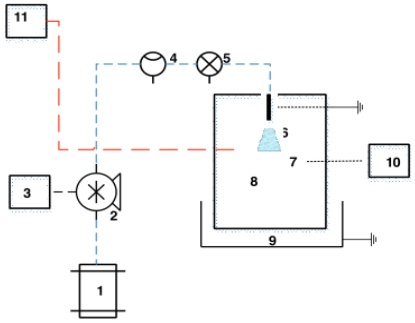

Figure 1: Flow sheet of experimental rig: 1 water tank, 2 Pump, 3 Inverter, 4 Flow meter, 5, Pressure gauge, 6 Spray, 7 Electrode, 8 Faraday Cage, 9 Water collector, 10 Electrometer, 11 HV power supply

Table 1: Performance data of tests nozzle)

			Q_L, L/min			
Nozzle Model	Spray angle θ, °	D_0, m	1 bar	2 bar	3 bar	4 bar
216.364	60	14	53	71	81	9
216.404	60	2	85	116	14	158

The break-up length and spray angle were used to estimate liquid sheet geometric parameters using Linearized Instability Sheet Atomization (LISA) model (Ashgriz, 2011). The model assumed that the liquid bulk was transformed into a liquid sheet subjected to a spatial and temporal instability in a form of a wavy disturbance due to the aerodynamic interaction between the liquid and its surrounding gas. The wave grew until to reach a critical wavelength at which the sheet broke into ligaments and, then, in large droplets. This first phase was called primary atomization. The formed droplets broke into smallest fragments due to disruptive aerodynamic forces (secondary atomization).

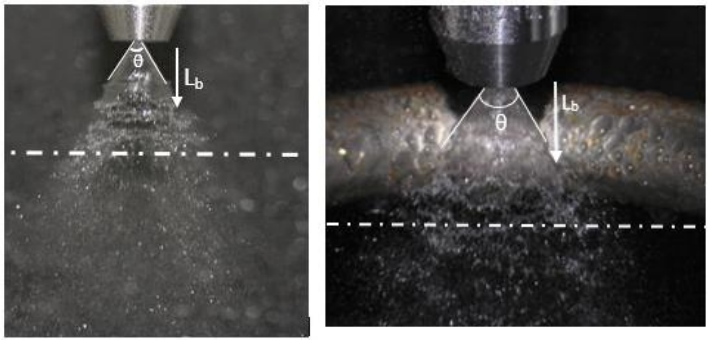

Figure 2: Breakup length and spray angle. In the pictures the Nozzle 1 at 3 bar is reported at 0 kV (left) and at V_{max} (right). The dotted line divides the primary and secondary atomization zones

In particular, the LISA model provides an estimation of the liquid sheet thickness that has a role in spray charging. Indeed, the model of Artana et al. (1993) considers the system liquid jet-electrode as an electrical circuit and assumes that the D-CMR is a function of Electric field intensity and sheet thickness *a* according to the formula:

$$\mathrm{D-CMR} = \frac{\varepsilon_0 \mathrm{E(V)}}{a}\left\{\frac{\varepsilon_0\varepsilon_r}{\sigma T_d}\left(1-\exp\left(\frac{-\sigma T_d}{\varepsilon_0\varepsilon_r}\right)\right)-1\right\} \quad (2)$$

where E is the electric field obtained from computational studies with COMSOL Multiphysics, ε_0 and ε_r are the vacuum and relative liquid permittivity respectively, σ is the liquid conductivity and Td is droplet formation time. Regarding that for water T_d<<1, Eq(2) can be simplified in the formula used in our investigation:

$$\mathrm{D-CMR} = \frac{\varepsilon_0\varepsilon_r E(V)}{a} \quad (3)$$

3. Experimental Results

In Figure 3, the droplets current I_{drop}, the D-CMR and the breakup length L_b for Nozzle 1 and 2 respectively are reported for both pressures.

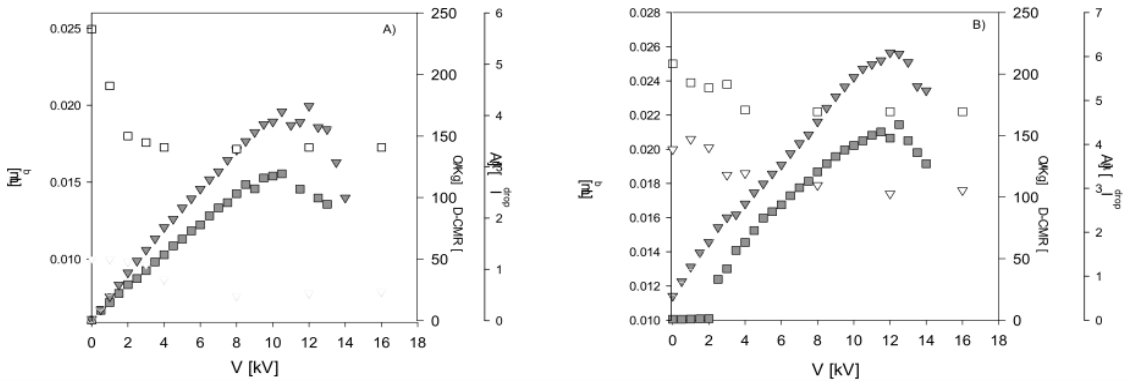

Figure 3: Comparison of Droplet charge to mass ratio, droplets current and breakup length at different voltages for Nozzle 1 (left) and 2 (right). Grey symbols: D-CMR/I_{drop}, white symbols: L_b. ▼: 6 bar; ■: 3 bar.

Regarding the trend of current and D-CMR, it can be observed that they increased almost linearly with a slope β as function of applied potential until to a maximum voltage called V_{max}, then they started to decrease. The highest charging levels were obtained at 6 bar for both nozzles. In this case, the highest current appeared when the liquid flow rate was higher. Indeed, the same trend was observed by comparing the behavior of two nozzles: an increase of 50 % of current for the nozzle 2 at V_{max} was measured. The breakup length showed a not negligible dependence on electric field. It decreased significantly and then from 8 kV it assumed a constant value. This behavior could be explained by assuming that the liquid sheet is perturbed by both aerodynamic and electric forces. The spray angle slightly increased by about 5 ° by increasing V because of repulsion of charge droplets.
Table 2 summarizes the main experimental results.

Table 2: Summary of experimental results

Nozzle	P [bar]	Q_L [L/min]	β 10^{-3} [1/Ω]	V_{max} 10^{-3} [V]	I_{max} 10^{-6} [A]	L_b (V_0) 10^{-2} [m]	L_b (V_{max}) 10^{-2} [m]	θ (V_0) [°]	θ (V_{max}) [°]
1	3	81	3	105	286	25	176	60	60
	6	116	39	12	418	1	75	60	65
2	3	14	40	125	445	25	22	60	60
	6	196	56	12	609	2	174	60	62

4. Discussion

The optical tests results were used to evaluate the atomization parameters following LISA model (Ashgriz, 2011). Starting from the optical evaluation of L_b, the half sheet thicknesses at exit (a_0) and breakup (a_b) points, the breakup time (τ_b) and the primary droplets diameter (d_D) were evaluated.

Table 3: Breakup parameters for both nozzles in uncharged conditions

Nozzle	P [bar]	a_0 10^{-4} [m]	a_b (V_0) 10^{-5} [m]	a_b (V_{max}) 10^{-5} [m]	d_D (V_0) 10^{-4} [m]	d_D (V_{max}) 10^{-4} [m]	τ_b (V_0) 10^{-3} [s]	τ_b (V_{max}) 10^{-4} [s]
1	3	23	249	311	661	723	113	897
	6	23	510	709	610	692	417	292
2	3	27	367	450	860	909	150	121
	6	27	437	564	580	630	890	681

By comparing the results, it was observed that the half sheet thickness a_0 increased with diameter d_0 and as consequence the larger a_0, the bigger half sheet thickness at breakup point. It is worth underlining that the thickness a_b and the breakup time followed the same trend of breakup length with pressure: as P increased, the liquid sheet broke earlier at a lower time and had a larger thickness. To take into account for the effect of charging potential on liquid sheet breakup, we introduced a dependence of surface tension on the droplet charge, while liquid density and viscosity were assumed as constant. The surface tension was calculated as a function of droplets experimental charge Q_D and its Rayleigh limit Q_R (Taflin et al., 1989) as follows (Tang, 1994):

$$\sigma_e = \sigma_L \left(1 - \frac{Q_D}{Q_r}\right) \tag{4}$$

It was varied with potential until V_{max}. Starting from the droplet diameter evaluated from LISA, the volume $V_D$was calculated. From V_D and D-CMR, the droplet charge and Rayleigh limit were known. The final values were estimated with an iterative calculation until to achieve an error less than 2 %.
The values of thickness a_b were used in the induction charging model to evaluate the theoretical D-CMR (Eq.3). For each potential from 0 kV to V_{max}, the sheet thickness was set as LISA value $a_b(V)$, while the electric field was evaluated along the direction of liquid sheet from nozzle exit to the actual breakup point. In Figure 4, the ratio the $D\text{-}CMR_{exp}$ and the $D\text{-}CMR_{th}$ is graphed.

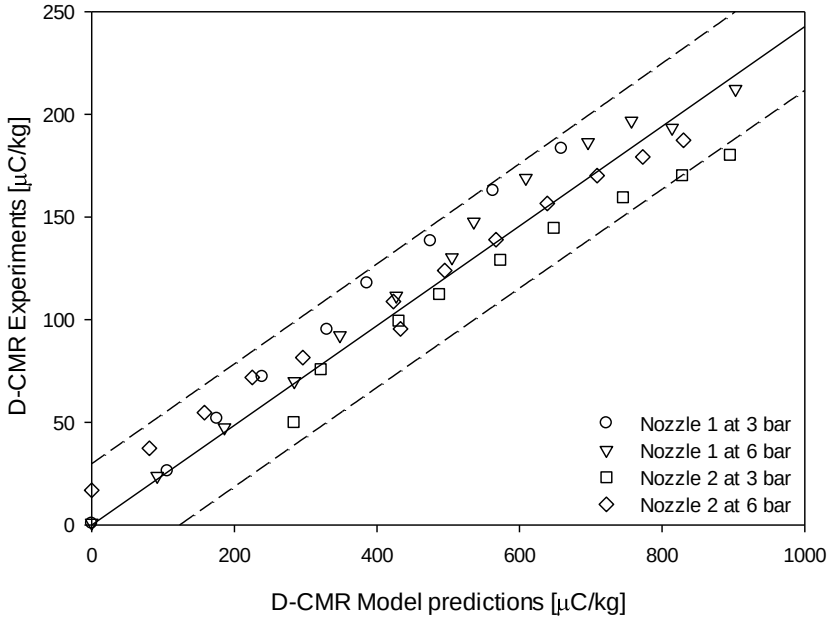

Figure 4: Comparison between theoretical and experimental droplet charge to mass ratio at different potential

It is worth to underline that experimental data of Nozzle 2 at 3 bar from 0 kV to 4 kV are not plotted because this evaluation is restricted to the linear range of D-CMR (V).
All data were fitted with a linear regression to estimate the slope that is the proportional factor between experimental and theoretical evaluations. The results of regression was a coefficient of $0.243 \pm 8.80 \cdot 10^{-3}$ and a coefficient of determination R^2 of 0.9364. It can be observed that all data are enclosed in a defined range. It implies that the model describes experimental values satisfactory.

5. Conclusions

In this work, a lab-scale electrified spray was studied in order to evaluate the charging level on liquid droplets charged by induction. We used 60 ° hollow cone hydraulic spray nozzles and a toroidal ring as induction charging electrode. The experiments were aimed to estimated break up length of the spray nozzles in uncharged and charged conditions and droplet charging efficiency as a function of the charging potential. At low potential the droplet charge to mass ratio (D CMR) increased linearly with the charging potential, V. Then a maximum D-CMR level was achieved at V_{max} and for $V>V_{max}$ D-CMR started to decrease.

For $V<V_{max}$, the induction charging model was used to describe data obtained from charging tests. It was found that the experimental data were well described by induction charging model and a corrective factor of 0.243 was necessary to have a perfect coincidence between them. To this end, future work may benefit for the implementation of further investigations on the electro-hydrodynamic of liquid jets to identify the parameters this proportionality is related to.

References

Artana G., Bassani L.C., Scaricabarozzi R., 1993. Specific charge of induction electrified sprays. Journal of Electrostatics, 29(2), 127–145.

Ashgriz N., 2011. Handbook of atomization and sprays: theory and applications,

Chaplin M., 2009. Theory vs Experiment: What is the Surface Charge of Water? Water Journal, 1, 1-28.

Cross J.A., Fowler J.C.W., Fu G., 2003. Electrostatic Enhancement of water sprays for coal dust suppression, Sydney, Australia.

D'Addio L., Di Natale F, Carotenuto C., Lancia A., 2013. A lab-scale system to study submicron particles removal in wet electrostatic scrubbers. Chemical Engineering Science, 97, 176–185.

D'Addio L., Di Natale F, Carotenuto C., Lancia A., 2014. Experimental analysis on the capture of submicron particles (PM0.5) by wet electrostatic scrubbing. Chemical Engineering Science, 106, 222–230.

Jaworek A, Krupa A., Balachandran W., Lackowski M., 2006. Multi-nozzle electrospray system for gas cleaning processes. Journal of Electrostatics, 64(3-4), 194–202.

Krupa A., Jaworek A., 2013. Charged spray generation for gas cleaning applications. Journal of Electrostatics, 71(3), 260–264.

Laryea G., No S., 2004. Spray angle and breakup length of charge-injected electrostatic pressure-swirl nozzle. Journal of Electrostatics, 60(1), 37–47.

Law S.E., 2001. Agricultural electrostatic spray application: a review of significant research and development during the 20th century. Journal of Electrostatics, 6, 25–42.

Law S.E., 1978. Embedded- Electrode Electrostatic-Induction Spray-Charging Nozzle: Theoretical and Engineering Design. Transactions of the ASAE, 21(6), 1096–1104.

Lechler, Lechler. <www.lechler.de/index-en_US> accessed 02.04.2016.

Di Natale F., Carotenuto C., D'Addio L., Jaworek A, Krupa A., Szudyga M., Lancia A., 2015. Capture of fine and ultrafine particles in a wet electrostatic scrubber. Journal of Environmental Chemical Engineering, 3(1), 349–356.

Di Natale F., Carotenuto C., D'Addio L., Lancia A., Antes T., Szudyga M., Jaworek A., Gregory D., Jackson M., Volpe P., Beleca R., Manivannan N., Abbod M., Balachandran W., 2013. New Technologies for Marine Diesel Engine Emission Control. Chemical Engineering Transaction, 32, 361–366.

Di Natale F., Carotenuto C., 2015. Particulate matter in marine diesel engines exhausts: Emissions and control strategies. Transportation Research Part D: Transport and Environment, 40, 166–191.

Taflin D.C., Ward T.L., Davis E.J., 1989. Electrified droplet fission and the Rayleigh limit. Langmuir, 5(2), 376–384.

Tang K., 1994. The Electrospray: Fundamentals and Feasibility of its Application to Targeted Drug Delivery by Inhalation.